ELSEVIER

PII: S0010-4485(98)00020-7

Computer-Aided Design, Vol. 30, No. 8, pp. 631–640, 1998

Printed in Great Britain
0010-4485/98/$19.00+0.00

Variable-feedrate CNC interpolators for constant material removal rates along Pythagorean-hodograph curves

Rida T. Farouki†*, Jairam Manjunathaiah†, David Nicholas†, Guo-Feng Yuan† and Sungchul Jee‡

An NC system that machines a curved shape at fixed depth of cut experiences time-varying cutting forces due to the 'curvature effect'—the material removal rate is higher than nominal in concave regions, and lower in convex regions. A curvature-dependent feedrate function that automatically compensates for this effect is formulated, and it is shown that, for Pythagorean-hodograph (PH) curves, the periodic real time computation of reference points in accordance with this function can be analytically reduced to a sequence of root-finding problems for simple monotone functions. Empirical results from an implementation of this variable-feedrate interpolators on an open-architecture CNC milling machine are presented and compared with results from fixed-feedrate interpolators. The curvature-compensated feedrate scheme has important potential applications in ensuring part accuracy and in optimizing part programs consistent with a prescribed accuracy.

Keywords: Pythagorean hodographs, CNC interpolators, feedrate, curvatures, osculating circle, offset curves, cutting force, machining accuracy

INTRODUCTION

The prevailing practice in CNC machining of complex shapes is to use G code part programs[22] in lieu of the *exact* tool path descriptions; this amounts to approximating the tool paths by linear/circular segments that are compatible with interpolators 'hard-wired' in the CNC system. The problem of driving machine tools directly from analytic curve definitions, by means of software interpolators in an 'open architecture' CNC system, has recently attracted much attention[2,3,20,21,23,26,27,30]. The proposed schemes, however, are also inherently approximate since they rely on truncated Taylor series—typically, only the linear term is retained—to generate the reference points* required by the control algorithm. Such methods are unsuited to curves with uneven parameter flow or curvature distributions, and they cannot be readily adapted to accommodate variable-feedrate specifications.

The *Pythagorean-hodograph* (PH) *curves* are a novel family of free-form parametric curves[15], compatible with the Bézier/B-spline representations of CAD systems, whose intrinsic algebraic structure allows the computational difficulties of free-form curve interpolators to be largely circumvented. In the present context, the key property distinguishing PH curves from 'ordinary' polynomial curves is the fact that their arc lengths, curvatures, and offsets depend *rationally* on the curve parameter. This permits an analytic reduction of certain integrals that express the distance travelled along a PH curve at constant or variable feedrate during one sampling interval of the CNC system. Consequently, one may formulate CNC interpolators for machining free-form curves that are extremely accurate, efficient, robust, and flexible.

The algorithmic details of PH curve CNC interpolators were described in Ref [16], and preliminary results from an implementation on an open-architecture CNC machine were reported in Ref [9]. Our emphasis here is on an interpolator that yields a particular curvature-dependent feedrate, motivated by practical machining issues. The cutting force exerted between the tool and workpiece is of primary concern in ensuring the accuracy of machined profiles—it influences tool deflection and wear, deformation of the workpiece, and heat generation. Limiting the cutting force within prescribed bounds is thus a key requirement for part accuracy and tool longevity.

*To whom correspondence should be addressed. Tel: +1 313 747-0081; Fax: +1 313 747-3170; E-mail: farouki@engin.umich.edu
†Department of Mechanical Engineering and Applied Mechanics, University of Michigan, Ann Arbor, MI 48109, USA
‡Department of Mechanical Engineering, Dankook University, 8 Hannam-Dong, Yongsan-Ku, Seoul 140-714, South Korea
Paper Received: 15 April 1997. Revised: 19 February 1998

* The reference points do lie exactly on the curve, but their distribution along it is not rigorously consistent with the specified feedrate—i.e., the tool path geometry is accurate, but the desired feedrate function is only approximately realized.

Varying material removal rates along a 2D tool path may be a significant source of cutting force variations. These varying rates could be incurred by a variable depth of cut—i.e., thickness of the material strip to be removed, perpendicular to the tool path—or even, in the case of fixed depth of cut, by non-linearity of the tool path through 'curvature' effects (see Section 3 below). Such variations in the volume removal rate may be effectively cancelled out by continuous compensatory feedrate adjustment using an 'intelligent' CNC interpolation algorithm. For the PH curves, in particular, the formulation of such algorithms is eminently tractable: the required reference points can be accurately and efficiently generated with very modest CPU resources.

The automatic selection of feedrates in accordance with the part geometry and corresponding tool paths has been the focus of earlier studies[18,28,29]. These variable feedrates have been implemented in the context of traditional G code descriptions, however, using a feedrate post-processor program that specifies the proper feedrate for each linear or circular segment of the cutting path[18]. The use of G code part programs entails sacrificing knowledge of the exact tool path curvature, and attempts to vary the feedrate to allow for curvature are thus unavoidably compromised (in fact, the curvature becomes infinite at the junctures of linear G code segments).

We shall adopt the following plan for the remainder of this paper. In Section 2, a brief synopsis of the distinguishing properties of PH curves is presented. A curvature-dependent feedrate function that, under appropriate conditions, yields constant volume removal rate at fixed depth of cut is formulated in Section 3, and it is shown that PH curves are admirably suited to a realization of this variable feedrate through a simple real-time interpolation algorithm. Speed and force measurements from an implementation of this interpolator on an 'open-architecture' CNC milling machine are presented in Section 4. Finally, in Section 5 we assess these results and identify avenues for further investigation.

PYTHAGOREAN-HODOGRAPH CURVES

We adopt the nomenclature and units used[9,16] in earlier studies, namely:

t = time (s),
s = curve arc length (mm),
ξ = curve parameter (dimensionless),
$\sigma = ds/d\xi$ = 'parametric speed' (mm),
κ = curvature (mm^{-1}),
$V = ds/dt$ = feedrate along curve ($mm\ s^{-1}$).

Given polynomials $u(\xi)$ and $v(\xi)$ without common non-constant factors and $m = \max(\deg(u),\deg(v)) \geq 1$, a regular PH curve $\mathbf{r}(\xi) = (x(\xi),y(\xi))$ of degree $n = 2m + 1$ is defined, modulo a choice of origin, by the hodograph

$$x'(\xi) = u^2(\xi) - v^2(\xi),\ \ y'(\xi) = 2u(\xi)v(\xi) \qquad (1)$$

These are elements of a *Pythagorean triple* of polynomials—they satisfy

$$x'^2(\xi) + y'^2(\xi) = \sigma^2(\xi)$$

$\sigma(\xi) = |\mathbf{r}'(\xi)| = u^2(\xi) + v^2(\xi)$ being the 'parametric speed' of $\mathbf{r}(\xi)$, i.e., the rate of change $ds/d\xi$ of arc length with respect to the parameter. The fact that σ is a polynomial in ξ means that the arc-length function $s(\xi)$ is also a polynomial. Furthermore, the curvature is given by the rational function

$$\kappa(\xi) = 2\frac{u(\xi)v'(\xi) - u'(\xi)v(\xi)}{\sigma^2(\xi)} \qquad (2)$$

Thus, for example, a PH quintic is obtained by substituting Bernstein-form quadratic polynomials

$$u(\xi) = u_0(1-\xi)^2 + u_1 2(1-\xi)\xi + u_2\xi^2,$$

$$v(\xi) = v_0(1-\xi)^2 + v_1 2(1-\xi)\xi + v_2\xi^2$$

into eqn (1) and integrating. The Bézier control points of this curve can then be expressed in terms of the coefficients u_0, u_1, u_2 and v_0, v_1, v_2 as

$$\mathbf{p}_1 = \mathbf{p}_0 + \frac{1}{5}(u_0^2 - v_0^2, 2u_0v_0),$$

$$\mathbf{p}_2 = \mathbf{p}_1 + \frac{1}{5}(u_0u_1 - v_0v_1, u_0v_1 + u_1v_0),$$

$$\mathbf{p}_3 = \mathbf{p}_2 + \frac{2}{15}(u_1^2 - v_1^2, 2u_1v_1) + \frac{1}{15}(u_0u_2 - v_0v_2, u_0v_2 + u_2v_0),$$

$$\mathbf{p}_4 = \mathbf{p}_3 + \frac{1}{5}(u_1u_2 - v_1v_2, u_1v_2 + u_2v_1),$$

$$\mathbf{p}_5 = \mathbf{p}_4 + \frac{1}{5}(u_2^2 - v_2^2, 2u_2v_2)$$

where $\boldsymbol{p}_0$ is an arbitrary integration constant. The quartic $\sigma(\xi)$ defining the parametric speed of this curve is specified by the Bernstein coefficients

$$\sigma_0 = u_0^2 + v_0^2,$$

$$\sigma_1 = u_0u_1 + v_0v_1,$$

$$\sigma_2 = \frac{2}{3}(u_1^2 + v_1^2) + \frac{1}{3}(u_0u_2 + v_0v_2),$$

$$\sigma_3 = u_1u_2 + v_1v_2,$$

$$\sigma_4 = u_2^2 + v_2^2$$

and the arc length $s(\xi)$ is the quintic corresponding to the indefinite integral of $\sigma(\xi)$—it has Bernstein coefficients

$$s_0 = 0 \text{ and } s_k = \frac{1}{5}\sum_{j=0}^{k-1}\sigma_j \text{ for } k = 1,\ldots,5$$

We focus on PH quintics here, since they are well-suited to practical design applications—the above formulae generalize readily to PH curves of other (odd) degrees. Complete details on the construction and manipulation of PH curves† may be found in the references [1,4–8,12,15,16].

The interpolator described below is specific to PH curves. As noted above, these curves are fully compatible with the Bézier/B-spline representations of CAD systems. Not all Bézier/B-spline curves are PH curves, however, and to

† We consider only the *polynomial* PH curves here. The *rational* PH curves[24,25] are less suitable for real-time CNC interpolation, since their arc lengths are not, in general, rational expressions in the curve parameter.

take full advantage of the latter it is essential that path planning (e.g., for complex surfaces) be done directly in terms of PH curve motions and associated feedrate functions. Preliminary results in this regard, for the case of contour machining, are described in Ref [17]; and in Ref [10] a system of G codes for describing PH curves and feedrate functions is presented. The latter is designed to be compatible with the established conventions for 'ordinary' (linear/circular) G codes, allowing the two to be freely mixed.

CURVATURE-DEPENDENT FEEDRATE

We now consider the formulation of a CNC interpolator capable of driving a machine tool along a Pythagorean-hodograph curve at a feedrate determined by the local curvature. The form of curvature dependence is selected so as to yield, at constant depth of cut, an (approximately) constant rate of volume removal. This is motivated by simple models of the milling process[18], in which the cutting force is proportional to the volume removal rate. Reduced variations of the cutting force are expected to yield machined profiles of enhanced dimensional accuracy and surface finish.

It is perhaps not obvious that, for curved paths, fixed feedrate and depth of cut do *not* imply a constant material removal rate (MRR). In 'concave' regions the remaining material strip curves around the tool, incurring higher MRR than for a linear cut, while in 'convex' regions it curves away from the tool, causing a lower MRR.‡ A quantitative description of this effect, which is primarily of interest for finish cuts on strongly-curved tool paths—i.e., the radius of curvature is comparable to the tool radius—is formulated below.

Feedrate function

Consider a tool path defined by the PH curve $\mathbf{r}(\xi)$ with tangent $\mathbf{t} = \mathbf{r}'/|\mathbf{r}'|$, normal $\mathbf{n} = \mathbf{t} \times \mathbf{z}$, and curvature $\kappa = |\mathbf{r}'|^{-3}(\mathbf{r}' \times \mathbf{r}'') \cdot \mathbf{z}$, where $\mathbf{z}$ is a unit vector orthogonal to the plane of $\mathbf{r}(\xi)$. We note that κ is negative or positive according to whether $\mathbf{n}$ points *toward* or *away from* the center of curvature. The desired part shape is described by the offset

$$\mathbf{r}_d(\xi) = \mathbf{r}(\xi) + d\mathbf{n}(\xi) \tag{3}$$

at distance d, the tool radius, from $\mathbf{r}(\xi)$. The material that is to be removed, at depth of cut δ, lies locally to the *right* of the curve (in the direction of $\mathbf{n}$) as we traverse it with ξ increasing. Thus, positive curvature corresponds to a 'concave' cut, and negative curvature to a 'convex' cut.

For feedrate V_0 and depth of cut δ, the volume removal rate along a linear path (assuming unit thickness) is simply $V_0\delta$. Consider now an anticlockwise circular path of radius r—an annular volume $\pi(r+d)^2 - \pi(r+d-\delta)^2$ is removed in time $2\pi r/V_0$ (*Figure 1*), and hence the rate of volume removal is $V_0\delta[1 + (d - \frac{1}{2}\delta)/r]$. Similarly, for a clockwise circular path, an annular volume $\pi(r-d+\delta)^2 - \pi(r-d)^2$ is removed in time $2\pi r/V_0$, corresponding to a rate $V_0\delta[1 - (d - \frac{1}{2}\delta)/r]$. Since κ is $1/r$ for the anticlockwise circle and $-1/r$ for the clockwise circle (and 0 for the linear path) we can express the material removal rate in all these instances as $V_0\delta[1 + \kappa(d - \frac{1}{2}\delta)]$.

‡ Physically, such MRR variations incurred by the tool path curvature will be manifested by larger/smaller material chips issuing from concave/convex tool path regions, when all machine parameters—feedrate, spindle speed, tool type, etc.—are held constant.

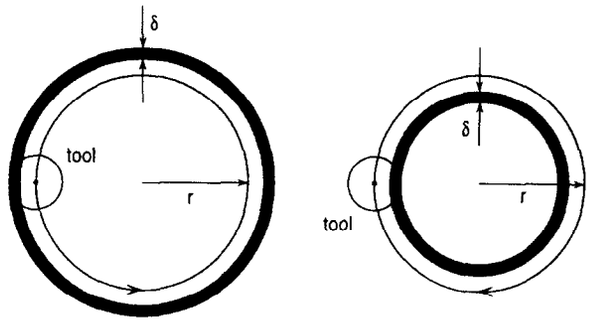

Figure 1 Annular volume removed (shaded regions) by a tool of radius d on a circular path of radius r with depth of cut δ. The anticlockwise path (left) defines an 'interior' cut, and the clockwise path (right) an 'exterior' cut

Consider now the PH curve $\mathbf{r}(\xi)$ as a tool path. Approximating this curve by its osculating circle at each point, we infer that 'curvature effects' incur a varying volume removal rate $V_0\delta[1 + \kappa(\xi)(d - \frac{1}{2}\delta)]$ along it, where $\kappa(\xi)$ is the curvature (eqn (2)) of $\mathbf{r}(\xi)$. Conversely, to maintain an approximately *constant* volume removal rate, the feedrate must be continuously varied in accordance with the curvature-dependent function

$$V(\xi) = \frac{V_0}{1 + \kappa(\xi)(d - \frac{1}{2}\delta)} \tag{4}$$

Note that $0 < d - \frac{1}{2}\delta < d$, since $0 < \delta < 2d$. In order for the offset curve (eqn (3)) to define a smooth part shape without self-intersections[11], the curvature of the path $\mathbf{r}(\xi)$ must satisfy $\kappa(\xi) > -1/d$ for $\xi \in [0,1]$. When this condition holds, eqn (4) yields a finite positive feedrate along the entire curve.

The variable feedrate (eqn (4)) deviates appreciably from the nominal value V_0 only when the curvature magnitude $|\kappa(\xi)|$ is not small compared to $1/(d - \frac{1}{2}\delta)$—i.e., when the (magnitude of the) radius of curvature of $\mathbf{r}(\xi)$ is not large compared to the tool radius d minus one-half the depth of cut δ. Assuming that $\delta \ll 2d$, this occurs at tight 'corners' in the tool path, of curvature magnitude comparable to $1/d$. Note that when $\delta = 2d$, the tool is always fully immersed and eqn (4) reduces to a constant feedrate.

A form equivalent to eqn (4) was previously suggested in Ref [16], though only as a means to avoid singularities in an inverse curvature feedrate specification: its physical basis (constant volume removal rate) was not recognized therein, and the formulation of interpolation algorithms was not pursued.

CNC interpolation algorithm

The simplest interpolators compute reference points corresponding to a fixed feedrate V_0 along a curve for a given sampling interval Δt. For a PH curve, this amounts to finding the unique real roots of the polynomial equations

$$s(\xi_k) = k\Delta s \quad \text{for } k = 1, 2, \ldots, \tag{5}$$

where $\Delta s = V_0\Delta t$. Taking the parameter value ξ_{k-1} of the preceding reference point as a starting approximation, a few Newton–Raphson iterations usually suffice. The Bernstein forms of $s(\xi)$ and its derivative $\sigma(\xi)$ are preferred for

numerical stability[13]—efficient evaluations may be obtained by writing (for a PH quintic)

$$s(\xi) = p^3(\tilde{s}_0 p^2 + \tilde{s}_1 pq + \tilde{s}_2 q^2) + (\tilde{s}_3 p^2 + \tilde{s}_4 pq + \tilde{s}_5 q^2)q^3$$

where $p = 1 - \xi$ and $q = \xi$ denote barycentric coordinates on $\xi \in [0,1]$ and $\tilde{s}_0, \ldots, \tilde{s}_5$ are *scaled* Bernstein coefficients[14], i.e., the appropriate binomial coefficients are absorbed into $s_0, \ldots, s_5$. Here p^2, pq, q^2 are to be computed only *once*; similar methods may be used for $\sigma(\xi)$ and $x(\xi)$, $y(\xi)$.

Now for the feedrate function defined by eqn (4) and sampling interval Δt, the parameter value ξ_k identifying the k-th reference point must satisfy

$$\int_0^{\xi_k} \frac{\sigma(\xi)}{V(\xi)}\, d\xi = k\Delta t \tag{6}$$

Substituting eqn (2) and eqn (4) into the above gives

$$(2d - \delta) \int_0^{\xi_k} \frac{u(\xi)v'(\xi) - u'(\xi)v(\xi)}{\sigma(\xi)}\, d\xi + \int_0^{\xi_k} \sigma(\xi)\, d\xi = kV_0\Delta t$$

and by writing $\phi(\xi) = v(\xi)/u(\xi)$ and noting that $\sigma(\xi) = u^2(\xi) + v^2(\xi) = s'(\xi)$, these integrals can be resolved to obtain the equation

$$F(\xi_k) = (2d - \delta)[\tan^{-1}\phi(\xi_k) - \tan^{-1}\phi(0)] + s(\xi_k) - kV_0\Delta t = 0 \tag{7}$$

This is a transcendental equation for ξ_k, which must be solved numerically. Note that $2\tan^{-1}\phi(\xi)$ is just the tangent-angle (measured from the x-axis) of the PH curve $\mathbf{r}(\xi)$. The treatment of the arctangent function in eqn (7) deserves special attention—if F is to be a continuous function, it is not permissible to simply take $-\pi/2 < \tan^{-1}\phi(\xi) \leq +\pi/2$ (say) for all ξ. Rather, we must add $j\pi$, where j is chosen among -1, 0, $+1$ so as to minimize§ the value of $|\tan^{-1}\phi(\xi_k) - \tan^{-1}\phi(\xi_{k-1}) + j\pi|$, to ensure continuity of F.

The integrand in eqn (6) is positive when $\kappa(\xi) > -1/d$ for $\xi \in [0,1]$ and F is then a *monotone* function—this guarantees that eqn (7) has a *unique* real root. The derivative of F can be written as

$$F'(\xi_k) = \sigma(\xi_k)[1 + \kappa(\xi_k)(d - \tfrac{1}{2}\delta)]$$

if, for example, Newton–Raphson iterations are used to determine its root. A good starting approximation for ξ_k is given by

$$\xi_k^{(0)} = \xi_{k-1} + \frac{V_0\Delta t}{\sigma(\xi_{k-1})[1 + \kappa(\xi_{k-1})(d - \tfrac{1}{2}\delta)]} \tag{8}$$

where ξ_{k-1} is the converged parameter value for the preceding reference point. Typically, a few iterations suffice for convergence of ξ_k to machine precision.

The total time T required to traverse the PH curve $\mathbf{r}(\xi)$ at the variable feedrate (eqn (4)) is obtained by integrating $\sigma(\xi)/V(\xi)$ from $\xi = 0$ to 1. This gives

$$T = \frac{S + 2\pi(d - \tfrac{1}{2}\delta)\Re}{V_0} \tag{9}$$

§ We assume that $V_0\Delta t$ is sufficiently small.

where the *rotation index* of $\mathbf{r}(\xi)$ is defined[12] by

$$\Re = \frac{1}{2\pi}\int_0^1 \kappa(\xi)\sigma(\xi)\, d\xi = \frac{\tan^{-1}\phi(1) - \tan^{-1}\phi(0)}{\pi} - I_0^1\phi(\xi)$$

Here, the Cauchy index $I_0^1\phi(\xi)$ of the rational function $\phi(\xi) = v(\xi)/u(\xi)$ on the interval $\xi \in [0,1]$ is equal[19] to the number of poles at which ϕ jumps from $-\infty$ to $+\infty$, minus the number at which it jumps from $+\infty$ to $-\infty$, as ξ increases from 0 to 1. It can be computed by inspecting the sign of the quantity $v(\xi)/u'(\xi)$ at each odd-multiplicity root of u on $(0,1)$.

Now T is not, in general, an integer multiple N of the sampling interval Δt. A traversal of the curve in a whole number of steps of duration Δt may be realized by modifying V_0 somewhat—namely, we take

$$N_* = \left\lfloor \frac{S + 2\pi(d - \tfrac{1}{2}\delta)\Re}{V_0\Delta t} + 0.5 \right\rfloor$$

steps at the feedrate (eqn (4)) with V_0 replaced by the slightly different value

$$\tilde{V}_0 = V_0 \frac{T}{N_*\Delta t}$$

Figure 2 shows the feedrate variation (eqn (4)) for a single PH quintic segment. We assume a tool radius $d = 0.125$ and depth of cut $\delta = 0.025$; the distance between the two curve endpoints is 1. Note how the feedrate falls to ~44% of the nominal value (for a straight cut) in the concave region of

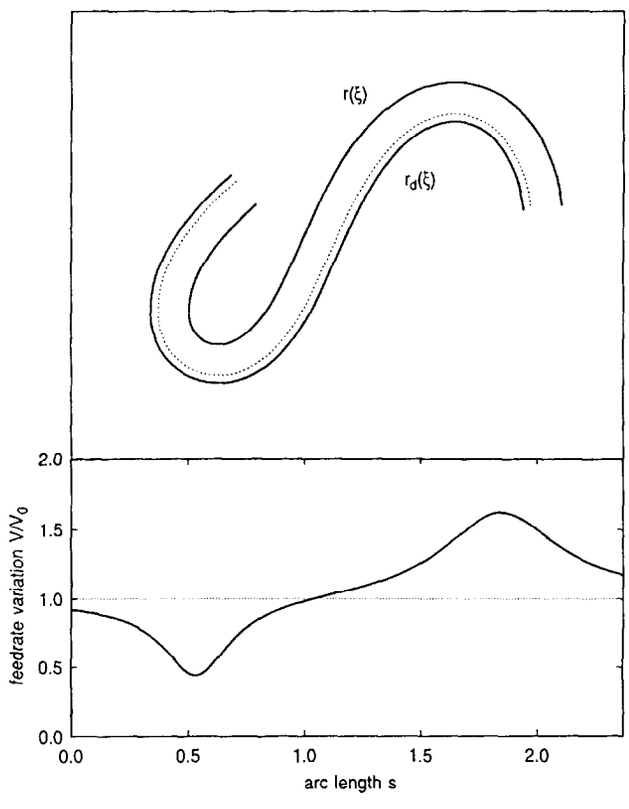

Figure 2 Feedrate variation along a PH-curve tool path in accordance with the curvature-dependent function (eqn (4)) to give a constant volume removal rate. Here $\mathbf{r}(\xi)$ is the PH quintic tool path, its offset $\mathbf{r}_d(\xi)$ is the desired part shape, and the dotted curve indicates the depth of cut above $\mathbf{r}_d(\xi)$ to be removed

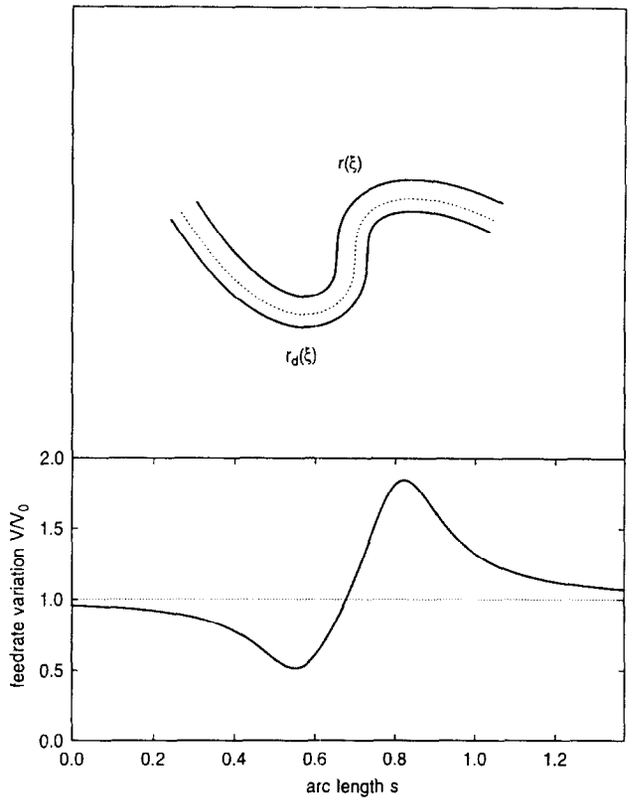

Figure 3 Another example of the feedrate function (eqn (4)) for a PH quintic

the curve, and subsequently grows to ~162% in the convex region.

A second PH quintic example is shown in *Figure 3*. Here we choose a tool radius $d = 0.1$ and depth of cut $\delta = 0.04$ (the distance between the curve endpoints is again 1). The feedrate dips to ~52% of V_0 in the concave region, and then rapidly climbs to ~185% of V_0 in the convex region. In *Figure 4* we illustrate the non-uniform sequence of reference points along this curve in accordance with the feedrate function (eqn (4)) and a fixed Δt, as generated by the interpolation algorithm described above.

Note that the geometrical model used to derive the feedrate function (eqn (4)) requires that the osculating circle be a 'sufficiently accurate' approximation to the curve at each point. A quantitative characterization of this condition is given in Appendix A—this can be checked to ensure that the feedrate (eqn (4)) will indeed give an (approximately) constant material removal rate.

The derivation of a more precise constant-MRR feedrate function would incur a far more cumbersome expression than eqn (4), and it is improbable that a rigorous real-time interpolation algorithm could be formulated for such a complicated feedrate dependence. From a practical perspective, it would not be warranted: we shall see below that the simple feedrate function (eqn (4)) easily cancels most of the machining-force variation under typical conditions. Note, however, that although eqn (4) will yield precisely constant MRR only under the conditions described in Appendix A, the actual realization of this feedrate variation by the CNC interpolator algorithm is essentially exact.

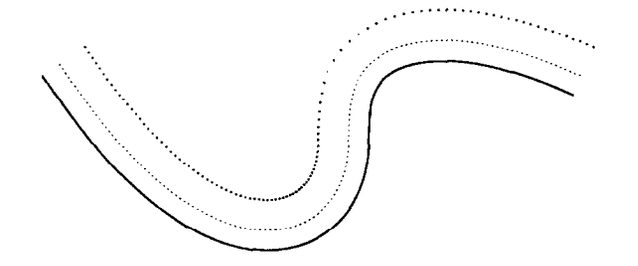

Figure 4 Non-uniform distribution of reference points along the PH quintic of *Figure 3* in accordance with the feedrate function (eqn (4)). The solid curve is the offset at the tool radius d, and the dashed curve shows the depth of cut

EXPERIMENTAL RESULTS

The experiments have been performed on a 3 hp CNC milling machine with interpolators implemented for two axes. To allow a detailed evaluation of the machine performance, the original control system was replaced by a 33 MHz 80486-based PC incorporating our own software interpolator and controller, and custom-made hardware components such as a pulse-width-modulation (PWM) board.¶ In addition, incremental linear encoders and tachometers are used to provide table position and motor speed feedback. The hardware components and control computer are interfaced through a digital I/O board, an analog-to-digital converter (ADC), and a quadrature decoder board. The system has a controller sampling interval of 0.01 s, and a basic length unit (BLU)—as defined by the position encoders—of 0.01 mm.

The controller compares instantaneous position measurements from the encoders with reference points generated by the interpolator. To emphasize the influence of the interpolation scheme (rather than the control algorithm) on the machine performance, a simple proportional (P) controller was used in the experiments. At each sampling time, the actual feedrate along the curve is the magnitude of the velocity vector whose components are measured by the tachometers. To compare with the specified feedrate variation, we must express the latter as a function of the elapsed time t, rather than the curve parameter ξ, as in eqn (4), or arc length s, as in *Figures 2 and 3*. This is accomplished—for plotting purposes, at least—by noting that, with the feedrate function (eqn (4)), t is given in terms of ξ by

$$t(\xi) = \frac{(2d - \delta)[\tan^{-1}\phi(\xi) - \tan^{-1}\phi(0)] + s(\xi)}{V_0} \qquad (10)$$

the arctangent function being interpreted in accordance with the convention previously described in Section 3.2 above.

In the CNC interpolator, just two Newton–Raphson iterations starting from the initial approximation (eqn (8)) were found to be more than adequate for real-time computation of the reference points to machine precision. Although eqn (7) involves a transcendental function, the calculations are easily within the scope of the modest (33 MHz) CPU used to control the CNC machine.

Tachometer measurements

Runs were performed on the two PH quintics shown in *Figures 2 and 3*—in each case, the distance between the

¶ Earlier experiments with this CNC system have been reported in Refs [9] and [23].

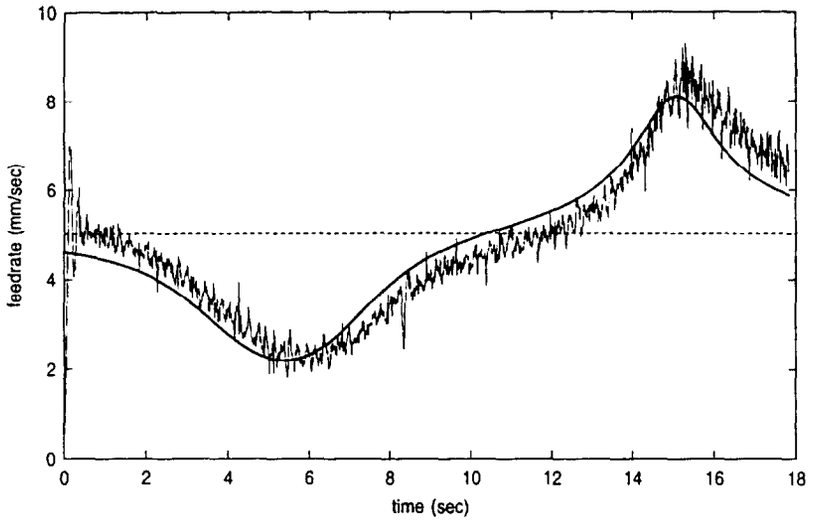

Figure 5 Measured time variation of feedrate for the PH quintic in *Figure 2*, from tachometer readings. The smooth curve illustrates the desired variation for a constant volume removal rate, as described by eqns (4) and (10)

curve endpoints was scaled to 3600 BLU (36 mm). In the first case a nominal (zero curvature) feedrate $V_0 = 5$ mm/s was chosen; for cutting parameters $(d,\delta) = (0.125,0.025)$ the quantity $d - \frac{1}{2}\delta$ is 405 BLU and the time (eqn (9)) needed to traverse the curve is $T = 17.82$ s In the second example, we take $V_0 = 4$ mm/s, and for $(d,\delta) = (0.1,0.04)$ we have $d - \frac{1}{2}\delta = 288$ BLU and $T = 12.75$ s The size of the curves and duration of the experiments are chosen to satisfy constraints on the memory available for real-time storage of encoder and tachometer readings.

Figure 5 compares the actual feedrate, as obtained from the tachometer readings, with the time-dependence of feedrate described by eqns (4) and (10) for the first example. The data shown here are from a single run—a comparison of results from several independent runs suggests that the observed fluctuations are primarily measurement noise rather than physical variations. Apart from the initial acceleration (and slight overshoot) from rest, the overall feedrate variation is seen to be in good agreement with eqn (4), although there does seem to be a small systematic lag between the expected and actual feedrate. The use of a more sophisticated control algorithm, and allowance for the initial acceleration period, will probably eliminate this discrepancy.

Figure 6 shows corresponding measurements for the PH curve in *Figure 3*. Although this example incurs much greater acceleration between the concave and convex portions of the curve, the system still faithfully reproduces the specified feedrate function. The discrepancy between the desired and actual feedrate variations does not appear to be simply a time lag in this case.

Note that the feed acceleration $A = \mathrm{d}V/\mathrm{d}t$ is obtained by applying $\mathrm{d}/\mathrm{d}t = (V/\sigma)\mathrm{d}/\mathrm{d}\xi$ to eqn (4)—this gives

$$A(\xi) = -\frac{V_0^2 \dot{\kappa}(\xi)(d - \frac{1}{2}\delta)}{[1 + \kappa(\xi)(d - \frac{1}{2}\delta)]^3} \tag{11}$$

where $\dot{\kappa}$ is the arc-length derivative of curvature; see eqn (16) in Appendix A. This is plotted in *Figure 7* for both curves.

Dynamometer measurements

To monitor machining force variations, a Kistler piezoelectric dynamometer was mounted on the machine table and used to record the x and y force components while cutting 6061-aluminum. For these experiments, the PH

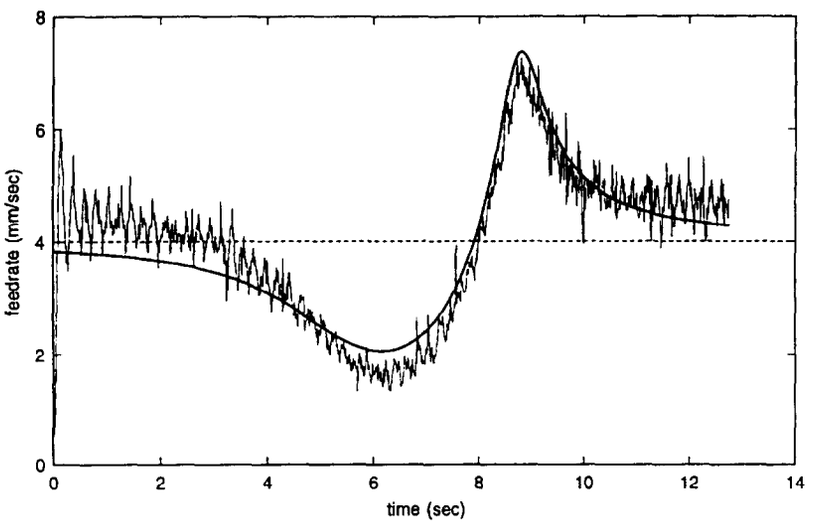

Figure 6 Measured time variation of feedrate for the PH quintic in *Figure 3*

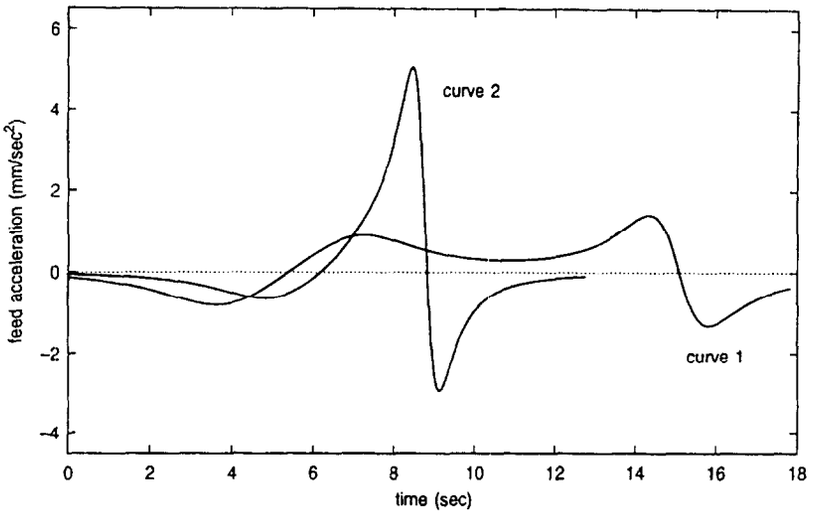

Figure 7 The feed acceleration (eqn (11)) for the PH quintics in *Figures 2 and 3*

quintic tool path shown in *Figure 3* was adopted, with the distance between the endpoints scaled to 2 inches (50.8 mm). The stock was first rough-cut using a $\frac{1}{2}$ inch diameter tool, leaving a $\frac{3}{16}$ inch depth of cut ($\delta = 4.76$ mm) above the desired part shape. The part was then finish-cut with the same tool ($d = 6.35$ mm) using PH-curve CNC interpolators for both the variable feedrate (eqn (4)) with $V_0 = 5$ mm/s, and a constant 5 mm/s feedrate.

A two-flute cutter and spindle speed of 1400 rpm were employed in these experiments, with an axial depth of cut ~3 mm into the aluminum stock. *Figure 8* shows the resultant force in the cutting plane, as measured by the dynamometer with a sampling frequency of 25 Hz. The spikes in these data represent successive engagements of the cutting edges with the workpiece. Since it is difficult to identify trends in the mean cutting force from the raw measurements, we also present moving averages of them—obtained with a 1-s 'sampling window'—in *Figure 8*.

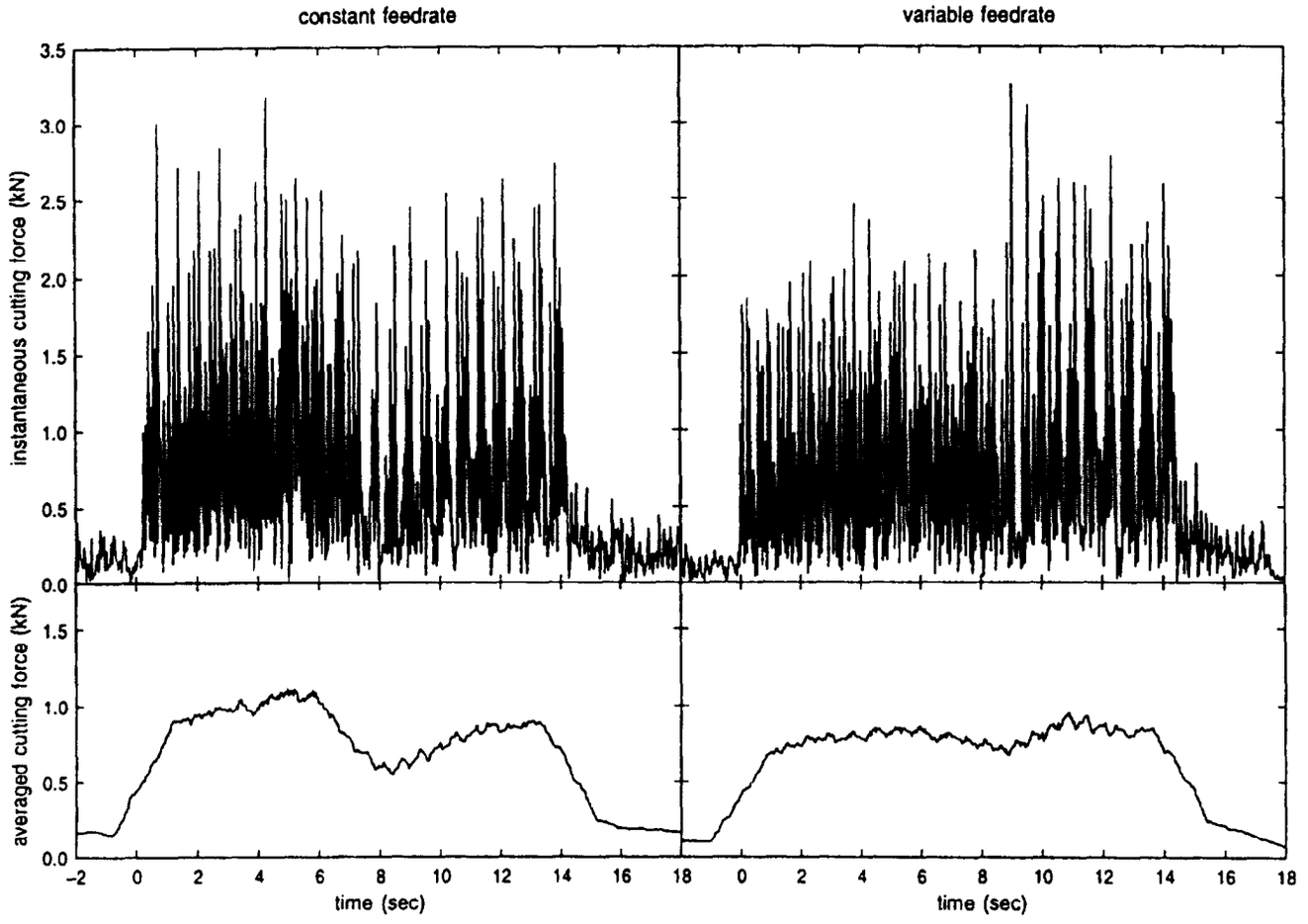

Figure 8 Measured cutting force for the PH quintic in *Figure 3* with: (left) fixed feedrate and (right) the curvature-dependent feedrate function (eqn (4)). The upper graphs indicate the instantaneous force in the cutting plane sampled at 25 Hz, and the lower graphs are 1-s moving averages of these data

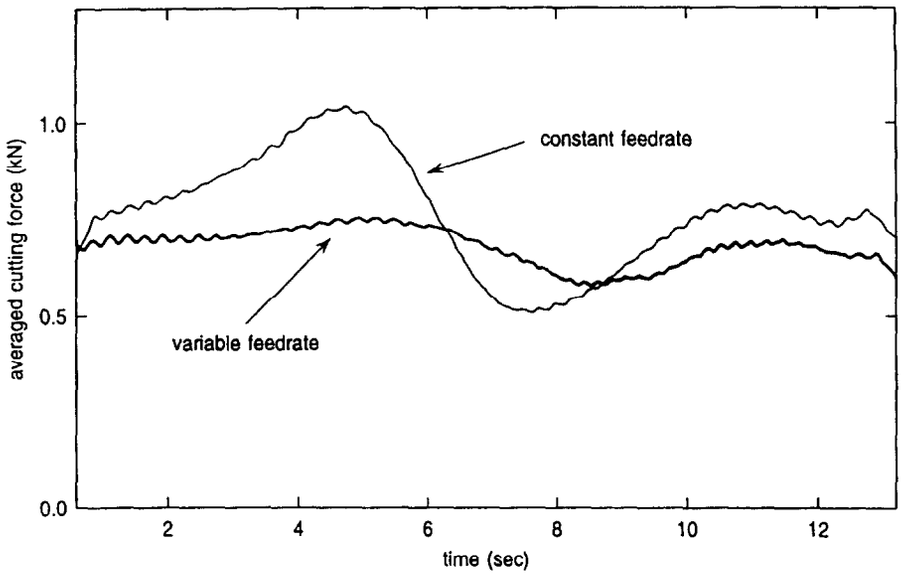

Figure 9 Averaged cutting force for the PH curve shown in *Figure 3*, based on a sampling frequency of 250 Hz and 1-s smoothing interval, for both a constant feedrate and the curvature-dependent feedrate function (eqn (4))

In the smoothed data for the constant feedrate case, an increase of the mean force on entering the 'concave' region of the curve in *Figure 3*, and a subsequent decrease when traversing the 'convex' region, is clearly apparent. In this case, the mean force varies by a factor of ~2. In the run with the feedrate function (eqn (4)), on the other hand, these variations are almost precisely cancelled out, and systematic fluctuations of the mean force are no more than ~10% about the nominal value (note that the initial 'rise' and final 'decay' in the averaged graphs are artifacts of the smoothing process).

The two-flute cutter and 1400 rpm spindle speed correspond to a 46.7 Hz frequency of engagement of the tool cutting edges with the workpiece. Since this exceeds the force-measurement sampling frequency of 25 Hz, one may be concerned that the data in *Figure 8* are influenced by aliasing effects. To verify that this is not so, the experiments were repeated using a 250 Hz sampling frequency. *Figure 9* shows the averaged data (with 1-s smoothing) from these runs, excluding the initial and final 1-s intervals. The trend is identical to that in *Figure 8*: the constant-feedrate run exhibits a substantial increase/decrease of mean cutting force in the concave/convex curve regions, while the variable feedrate (eqn (4)) effectively cancels out these variations.

CONCLUDING REMARKS

We have shown that PH curves admit the formulation of simple real-time CNC interpolators that compensate for varying material removal rates at a fixed depth of cut through curvature-dependent feedrates. The performance of these interpolators has been verified through implementation on an open architecture‖ CNC milling machine. The curvature-dependent feedrate was accurately realized using a simple P control algorithm, and it effectively cancelled variations of the mean cutting force due to 'curvature effects' when machining aluminum at fixed depth of cut.

‖ The implementation of this PH curve interpolator does not, in fact, require a fully open-architecture system—it is only necessary that the software interface between the interpolator and control algorithm be clearly specified and accessible.

The control over machining forces afforded by this interpolator is expected to provide improvements in the surface finish and dimensional accuracy of precision machined parts. This is accomplished by low-level software changes in the control computer, based on the tool-path geometry, without the need for addition of sophisticated sensors or complex control algorithms. Although we have considered only variations in the material removal rate due to varying curvature at a fixed depth of cut, it is also possible to formulate PH-curve interpolators that compensate for specified variable depth-of-cut functions. Finally, note that the variable-feedrate capability of PH-curve interpolators—see also Ref [9] and Ref [16]—may prove valuable in optimizing overall machining times for part programs, consistent with specified constraints on machining forces, part accuracy, and surface finish.

ACKNOWLEDGEMENTS

We are grateful to Professor Yoram Koren for advice and encouragement. This work was supported by the National Science Foundation (CCR-9530741) and the Office of Naval Research (N00014-95-1-0767).

APPENDIX A: OSCULATING-CIRCLE APPROXIMATION

The feedrate function (eqn (4)) for constant material removal rate is based on local approximation of the curve by its osculating circle, and is valid only if this approximation is sufficiently accurate over lengths comparable to the tool radius. We now derive a quantitative characterization of this condition.

An analytic curve can be developed in a power series in its arc length s measured from a chosen point $\mathbf{r}_0$ with tangent $\mathbf{t}_0$ and normal $\mathbf{n}_0$ as

$$\mathbf{r}(s) - \mathbf{r}_0 = \left(s - \frac{\kappa_0^2}{6}s^3 + \dots\right)\mathbf{t}_0 - \left(\frac{\kappa_0}{2}s^2 + \frac{\dot{\kappa}_0}{6}s^3 + \dots\right)\mathbf{n}_0 \tag{12}$$

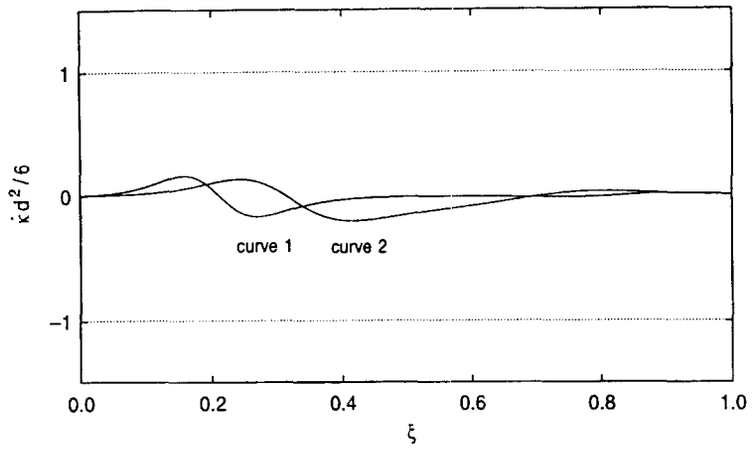

Figure 10 Verification of the inequality (eqn (15)), describing the accuracy of the osculating-circle approximation, for the PH curves shown in *Figures 2 and 3*

where κ_0 and $\dot{\kappa}_0$ denote the curvature and its arc-length derivative at $\mathbf{r}_0$. Now the osculating circle at $\mathbf{r}_0$ has radius $\rho_0 = 1/\kappa_0$ and center $\mathbf{r}_0 - \rho_0\mathbf{n}_0$, and is thus described by $\mathbf{c}(s) = \mathbf{r}_0 + \rho_0 \sin\theta\mathbf{t}_0 - \rho_0(1 - \cos\theta)\mathbf{n}_0$ with $\theta = s/\rho_0 = \kappa_0 s$. Expanding trigonometric terms in power series, we obtain

$$\mathbf{c}(s) - \mathbf{r}_0 = \left(s - \frac{\kappa_0^2}{6}s^3 + \ldots\right)\mathbf{t}_0 - \left(\frac{\kappa_0}{2}s^2 - \frac{\kappa_0^3}{24}s^4 + \ldots\right)\mathbf{n}_0 \tag{13}$$

Comparing eqns (12) and (13), we see that the deviation between points of equal arc length s from $\mathbf{r}_0$ along the osculating circle and the given curve is

$$\mathbf{c}(s) - \mathbf{r}(s) = \frac{\dot{\kappa}_0}{6}s^3\mathbf{n}_0 + O(s^4) \tag{14}$$

The tool 'samples' $\mathbf{r}(\xi)$ on a length scale $\sim d$. Thus, as a rough criterion that the osculating circle at each point satisfactorily approximates the curve, we require that $|\mathbf{c}(s) - \mathbf{r}(s)| \ll d$ for $s \leq d$. This gives the condition

$$\frac{1}{6}|\dot{\kappa}_0|d^2 \ll 1 \tag{15}$$

where, in terms of the polynomials $u(\xi)$ and $v(\xi)$, we have

$$\dot{\kappa} = \frac{\kappa'}{\sigma} = \frac{2(u^2+v^2)(uv'' - u''v) - 8(uu' + vv')(uv' - u'v)}{(u^2+v^2)^4} \tag{16}$$

Note, however, that at a *vertex* (a point of extremum curvature), $\dot{\kappa} = 0$ and the deviation of $\mathbf{r}(\xi)$ from its osculating circle is described by the higher-order terms in eqn (14)—these are typically of much smaller magnitude.

To be confident that the feedrate function (eqn (4)) does yield an approximately constant volume removal rate along the PH-curve tool path, one must check that the inequality (eqn (15)) is satisfied along the curve. *Figure 10* shows that this condition does indeed hold for the PH quintics in *Figures 2 and 3*.

REFERENCES

1. Albrecht, G. and Farouki, R. T., Construction of C^2 Pythagorean-hodograph interpolating splines by the homotopy method. *Advances in Computational Mathematics*, 1996, **5**, 417–442.
2. Chou, J.-J. and Yang, D. C. H., Command axis generation for three-axis CNC machining. *ASME Journal of Engineering for Industry*, 1991, **113**, 305–310.
3. Chou, J.-J. and Yang, D. C. H., On the generation of coordinated motion of five-axis CNC/CMM machines. *ASME Journal of Engineering for Industry*, 1992, **114**, 15–22.
4. Farouki, R. T., Pythagorean-hodograph curves in practical use. In *Geometry Processing for Design and Manufacturing*, ed. R. E. Barnhill. SIAM, Philadelphia, 1992, pp. 3–33.
5. Farouki, R. T., The conformal map $z \rightarrow z^2$ of the hodograph plane. *Computer Aided Geometric Design*, 1994, **11**, 363–390.
6. Farouki, R. T., The elastic bending energy of Pythagorean-hodograph curves. *Computer Aided Geometric Design*, 1996, **13**, 227–241.
7. Farouki, R. T., Pythagorean-hodograph quintic transition curves of monotone curvature. *Computer-Aided Design*, 1997, **29**, 601–606.
8. Farouki, R. T., Manjunathaiah, J. and Jee, S., Design of rational cam profiles with Pythagorean-hodograph curves. *Mechanism and Machine Theory*, 1998, to appear.
9. Farouki, R. T., Manjunathaiah, J. and Jee, S., Implementation and performance analysis of a real-time CNC interpolator for precision machining of Pythagorean-hodograph curves. *ASME Journal of Manufacturing Science and Engineering*, 1997, submitted.
10. Farouki, R. T., Manjunathaiah, J. and Yuan, G.-F., G codes for the specification of Pythagorean-hodograph tool paths and associated feedrate functions on open-architecture CNC machines. *International Journal of Machine Tools and Manufacture*, 1998, to appear.
11. Farouki, R. T. and Neff, C. A., Analytic properties of plane offset curves, Algebraic properties of plane offset curves. *Computer Aided Geometric Design*, 1990, **7**, 83–127.
12. Farouki, R. T. and Neff, C. A., Hermite interpolation by Pythagorean-hodograph quintics. *Mathematics of Computation*, 1995, **64**, 1589–1609.
13. Farouki, R. T. and Rajan, V. T., On the numerical condition of polynomials in Bernstein form. *Computer Aided Geometric Design*, 1987, **4**, 191–216.
14. Farouki, R. T. and Rajan, V. T., Algorithms for polynomials in Bernstein form. *Computer Aided Geometric Design*, 1988, **5**, 1–26.
15. Farouki, R. T. and Sakkalis, T., Pythagorean hodographs. *IBM Journal of Research and Development*, 1990, **34**, 736–752.
16. Farouki, R. T. and Shah, S., Real-time CNC interpolators for Pythagorean-hodograph curves. *Computer Aided Geometric Design*, 1996, **13**, 583–600.
17. Farouki, R. T., Tsai, Y.-F. and Yuan, G.-F., Contour machining of free-form surfaces with real-time PH curve CNC interpolators. *Computer Aided Geometric Design*, 1998, to appear.
18. Fussel, B. K., Ersoy, C. and Jerard, R. B., Computer generated CNC machining feed rates. In *Proceedings of the Japan/USA Symposium on Flexible Automation*, Vol. 1, ASME, 1992, pp. 377–383.
19. Henrici, P., *Applied and Computational Complex Analysis*, Vol. 1. Wiley, New York, 1974.
20. Huang, J.-T. and Yang, D. C. H., A generalized interpolator for command generation of parametric curves in computer-controlled machines. In *Proceedings of the Japan/USA Symposium on Flexible Automation*, Vol. 1, ASME, 1992, pp. 393–399.
21. Koren, Y., Interpolator for a computer numerical control system. *IEEE Transactions on Computers*, 1976, **C-25**, 32–37.
22. Koren, Y., *Computer Control of Manufacturing Systems*. McGraw-Hill, New York, 1983.
23. Lin, R.-S. and Koren, Y., Real-time interpolators for multi-axis CNC machine tools. *Manufacturing Systems*, 1996, **25**, 145–149.

24. Pottmann, H., Rational curves and surfaces with rational offsets. *Computer Aided Geometric Design*, 1995, **12**, 175–192.
25. Pottmann, H., Curve design with rational Pythagorean-hodograph curves. *Advances in Computational Mathematics*, 1995, **3**, 147–170.
26. Sata, T., Kimura, F., Okada, N. and Hosaka, M., A new method of NC interpolation for machining the sculptured surface. *Annals of the CIRP*, 1981, **30**, 369–372.
27. Shpitalni, M., Koren, Y. and Lo, C. C., Realtime curve interpolators. *Computer-Aided Design*, 1994, **26**, 832–838.
28. Sungurtekin, U. A., Voelcker, H. B., Graphical simulation and automatic verification of NC machining programs. In *Proceedings of the IEEE International Conference on Robotics and Automation*, Vol. 1, San Francisco, 1986, pp. 156–165.
29. Vann, C. S. and Cutkosky, M. R., Closing the loop in CAD/CAM integration. In *Proceedings of the Japan/USA Symposium on Flexible Automation*, Vol. 2, ASME, 1988, pp. 915–922.
30. Yang, D. C. H. and Kong, T., Parametric interpolator versus linear interpolator for precision CNC machining. *Computer-Aided Design*, 1994, **26**, 225–234.

Rida T Farouki is a Professor in the Dept. of Mechanical Engineering and Applied Mechanics, University of Michigan, Ann Arbor. Formerly, he worked at the IBM Thomas J. Watson Research Center (1986–1994) and GE Corporate Research and Development (1983–1986). He received a PhD in astrophysics from Cornell University in 1983 and a BA in engineering science from Oxford University in 1978. Farouki is the author of papers in a variety of scientific and engineering disciplines, including computer-aided geometric design, numerical analysis, plasma physics, molecular dynamics, geometrical optics, and astrophysics.

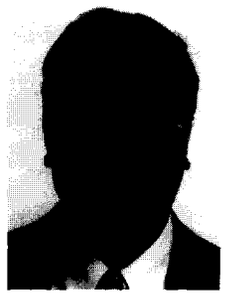

Jairam Manjunathaiah is a doctoral candidate in the Dept. of Mechanical Engineering and Applied Mechanics, University of Michigan, Ann Arbor. He received his Bachelor's degree in mechanical engineering from the Karnataka Regional Engineering College, Suratkal, India in 1992, and his Master's degree in manufacturing engineering from the University of Massachusetts, Amherst in 1995. His research interests include machine tools, manufacturing processes, and CAD/CAM. Manjunathaiah is an Associate Member of the Society of Manufacturing Engineers and a member of Pi Tau Sigma, the Mechanical Engineering Honor Society.

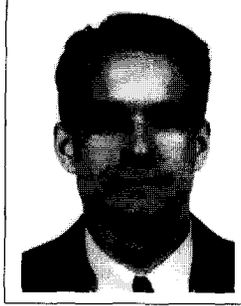

David Nicholas works in the Advanced Manufacturing Center of General Motors, Delphi Saginaw Steering Systems. He received a BSE in mechanical engineering and a BSE in materials science and engineering from the University of Michigan, Ann Arbor in 1997. His primary interests are in high-volume machining, metal forming, and heat treatment.

Guo-Feng Yuan is a graduate student in the Dept. of Mechanical Engineering and Applied Mechanics, University of Michigan, Ann Arbor. He received a BS in agricultural machinery engineering from National Taiwan University in 1993. Formerly, he was a full-time teaching assistant at the National Taiwan University (1995–1996), assisting in teaching engineering drawing, programming, and CNC machining. His research interests include computer-aided geometric modeling and design, CNC machining, and computer-controlled machines.

Sungchul Jee is currently a full-time Lecturer in the Dept. of Mechanical Engineering at Dankook University, Seoul, Korea. He received a PhD in mechanical engineering from the University of Michigan, Ann Arbor, in 1996, and an MS and BS in mechanical design and production engineering from Seoul National University, Seoul, Korea in 1990 and 1988, respectively. From 1996 to 1997 he worked as a Research Fellow in the Dept. of Mechanical Engineering and Applied Mechanics at the University of Michigan. His research interests include CNC servo controls and interpolators, fuzzy logic control systems, and open-architecture machining systems.